

Water Saturation Evaluation in a Fresh Brine Shaly Sand Reservoir

*Rob T. Wittebrood, Wittebrood Petrophysical Services Inc.
Hycal Energy Research Laboratories Ltd.*

Abstract

In reservoirs with fresh brine the effects of clay minerals are much larger than in more saline brine reservoirs. An evaluation of a very large shaly sand reservoir is presented, where the shale conducts up to 30 times more of the electricity than the brine. A reliable interpretation model was found by adjusting the standard Waxman-Smits model. By comparison it was found that the Dual Water model is incorrect. This adapted evaluation model is based on an extensive set of laboratory measurements. The upper and lower Aeolian sands could be evaluated consistent with Capillary Pressure data, whereas the middle Marine sands were more difficult to evaluate, due to different clay distributions and variable R_w values.

1.0 Introduction.

Shaly Sand reservoirs have challenged petrophysicists for over sixty years. To calculate the water saturation from resistivity logs the analyst need to correct for the additional electrical conductivity from the clay minerals. When the reservoir brine is relatively fresh, the evaluation problem is compounded, because the effect of the clay minerals is proportional to the resistivity of the brine. To assist the analyst in the calculation of the water saturation a spectre of more than thirty shaly-sand models have been introduced over the years. A large number of these evaluation models have been aptly classified by Worthington [1]. No single model has proven to be the panacea for all shaly sand reservoirs. Most of these models have been applied in more saline reservoirs ($R_w < 0.5 \Omega m$). Few excursions have been made into fresh water brines ($R_w > 0.5 \Omega m$). In this paper we consider a reservoir with $R_w = 5 \Omega m$, in which the effect of the clay conductivity can be a factor of ten or more larger than the brine conductivity. When the amount of clay is substantial, we will measure low resistivities, while the layer still may produce clean oil.

2.0 Reservoir Description.

The reservoir has an areal extent of well over 100 km² and a cumulative thickness of over 300 m. There are several parallel partly sealing thrust faults. Some wells intersect a small gas cap. Some wells penetrate below the free water level, which appears to be tilted. Most of the wells are not cored. The sand members do vary with depth. The top and bottom sands are of Aeolian origin. These Aeolian sands contain mainly authogenic dispersed clays and have an average porosity of 25%.

The middle sands are of Marine origin. These sands have authogenic dispersed clays, allogenic shale laminae and some structural shale grains. They have a porosity of around 20%. One sand member is rather silty with shale laminae containing substantial amounts of glauconite. Brine resistivity at the formation temperature of 80 °C is about 5 Ωm . The brine appears to be of meteoric origin. The composed brine only needed CaCl₂ and NaHCO₃, but no additional NaCl.

3.0 Evaluation of the Reservoir.

The routine evaluation of the reservoir led to significant discrepancies and inconsistencies. It was decided to resolve these problems with a large tangible set of laboratory measurements, including electrical properties and capillary pressure measurements.

The major issues to be resolved in the evaluation are:

OOIP :	variable Original Oil In Place
Sw:	inconsistent Water Saturation
Swirr :	large Irreducible Water Saturation
GOC:	different Gas Oil Contact levels
FWL:	tilted Free Water Level
H:	uncertain cut-offs for Pay
Rw:	variable brine Resistivity
Vcd:	amount and type of clay present
Qv:	Cation Exchange Capacity

4.0 Shaly Sand Evaluation Model.

A series of papers by Waxman, Smits and Thomas [2] form the peripety in shaly sand evaluation. They introduced a shaly sand model (Waxman-Smits model or WS-model) based on a strongly simplified physical concept, a solid electro-chemical basis and an extensive set of carefully executed experiments on samples containing various amounts of dispersed clays of different composition. This data set is by far the highest quality and most extensive data set available in the shaly sand literature. The same data set was also used in a paper by Clavier, Coates and Dumanoir [3]. They introduced, more than 15 years later, the Dual-Water model (or DW-model). In the DW-model a layer of bound-water, associated with the clay minerals, is considered. The resistivity of the clay bound water is different from the bulk water. These two models are the most frequently used models.

The current reservoir was routinely evaluated using the DW-model. However, inconsistent Water Saturation values led to ad hoc adjustments in the parameters of the DW-model.

5.0 The DW-model and WS-model.

The WS-model and the DW-model both are parallel conduction models. Which means, that the brine and the clay both conduct the current in parallel, with no further interaction between the two. It is also assumed that both current paths have exactly the same shape: Both models can be written for 100% brine saturated rock as:

$$C_O = (C_W + C_{CLAY})/F \quad (1)$$

with

- C_O : rock conductivity ($S_w=1$)
- C_W : brine conductivity
- C_{CLAY} : clay conductivity
- F : Formation Factor

In analogy with Archie we write usually:

$$F = 1/\phi^m \quad (2)$$

with

- ϕ porosity
- m cementation factor

The formation factor is a purely geometrical factor. Both clay and brine have the same formation factor in the two models. This means that water and clay are assumed to have the same geometry. So both are assumed to fill the total pore space, and indeed, the clay is implicitly assumed to be fully dispersed. Usually equation (1) is written in terms of resistivity rather than conductivity with $R=1/C$, or:

$$R_O/R_W = F/(1 + X) \quad (3)$$

with

- R_O resistivity of rock with $S_w=1$
- R_W resistivity of brine
- X clay effect = C_{CLAY}/C_W

In both models the clay effect can be written as:

$$X = R_W B Q_V \quad (4)$$

with

- B : counter ion mobility
- Q_V : Cation Exchange Capacity (per unit of pore volume)

For rock in which the water saturation is less than 100%, both models can be written as:

$$R_t/R_w = I \cdot F/(1 + X/S_w) \quad (5)$$

with

- I Resistivity Index
- S_w Water Saturation

At the formation temperature of 80 °C, we have $B= 8$, $R_w=5$. So when $Q_V=0.25$ (not high), we find $X = 5 \cdot 8 \cdot 0.15 = 10$. So in this case the clay conducts ten times more current than the brine. When the water saturation drops to 30%, the clay conducts 33 times more current than the brine. So, in fresh brines we may be looking at huge corrections for the effects of the clay.

The equivalence of the two models is shown in Appendix A. To distinguish between the two models different annotations are used.

For the WS-model:

$$R_O/R_W = F^*/(1 + R_W B^* Q_V) \quad (6)$$

with

$$F^* = 1/\phi^{m^*} \quad (7)$$

And for the DW-model:

$$R_O/R_W = F_O/(1 + R_W B_O Q_V) \quad (8)$$

with

$$F_O = 1/\phi^{m_o} \quad (9)$$

The only difference between the two models the parameter B , the counter ion mobility. The counter ion mobility is the crux of the model and is calculated differently for both models.

The WS-model uses:

$$B^* = 3.83 \cdot \{1 - 0.83 \cdot \exp(-0.5/R_W)\} \quad (10)$$

The DW-model uses:

$$B_O = 2.05 - \gamma/R_W \quad (11)$$

with

$$\begin{aligned} \gamma &= 0.3 & R_W < 0.3 \\ \gamma &= 0.3 + 0.432 \cdot \{(R_W - 0.3)^{2/3}\} & R_W > 0.3 \end{aligned}$$

Equation (11) does not appear as such in the paper introducing the Dual Water model (Ref. 3), but in Appendix A it is shown that equation (11) follows immediately by rewriting the DW-model equation. The value of γ has been calculated by fitting a curve to the measurements provided in Reference (3).

The counter ion mobilities B^* and B_O are only a function of R_w and T (temperature). They are shown as a function of R_w in Figure 1. B^* gradually decreases with R_w from about 3.8 at low R_w to about 0.8 at high R_w . At low R_w , B_O is strongly negative. At $R_w=0.15 \Omega m$ it becomes zero, indicating that the clay bound water has the same resistivity as the bulk water. At high R_w , B_O keeps on increasing slowly. At $R_w=1.5 \Omega m$ B^* and B_O are equal and the two models would of course give identical results. So the behaviour of the two models as a function of R_w is distinctly different. The clay effect is described by the term $R_w B Q_V$, a comparison of $R_w B$ for the two models is less dramatic than Figure 1 suggests.

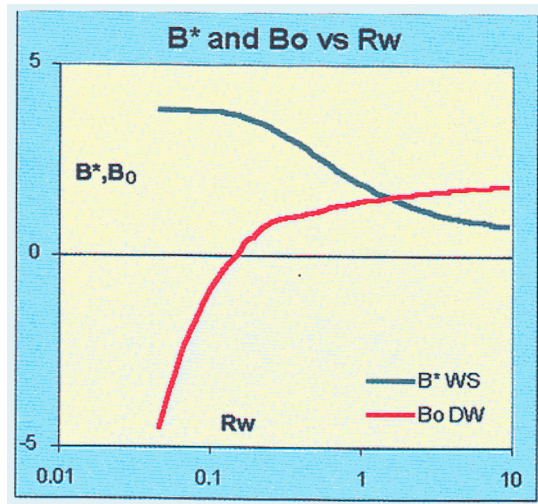


Figure 1: B^* and B_0 versus R_w .

6.0 Comparison of the DW- and WS-models.

6.1 Cementation exponents

The value of R_0/R_w is measured from experiments and is of course the same in equations (6) and (8). So, when the value of B is different in both models, the value of F also has to be different for both models. This means that the cementation exponents m^* and m_0 have to be different too.

When Q_v equals zero, there is no shale term X for both models. This means that m^* and m_0 are equal. When Q_v is greater than zero, the shale term X is different in both models and we should be able to see which model gives the most consistent value for the cementation factor m . The results shown in Figure 2 are for the upper Aeolian Sandstone.

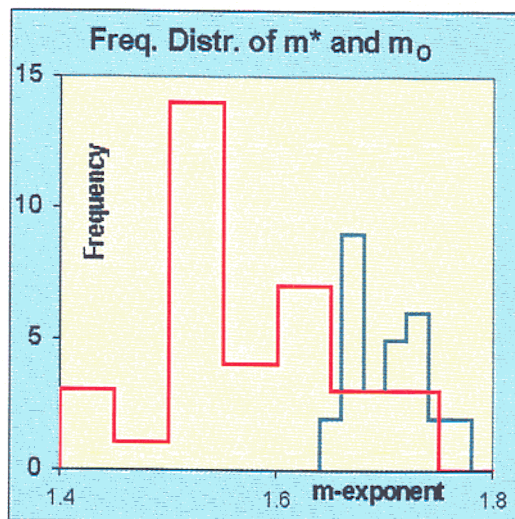


Figure 2: m -factor distribution for the Waxman-Smits model and the Dual Water model.

The value of Q_v as used, was determined from R_0 measurements at two salinities i.e. $R_w=1.5$ and $5.0 \Omega m$. Figure 1 shows that at $R_w=1.5 \Omega m$ the B_0 and B^* are actually equal and the calculated shale effect is the same for both models. At $R_w=5.0 \Omega m$ B_0 is twice as large as B^* . From the two R_0 measurements and the B -values as given, we may calculate Q_v and the cementation factor (m) for the sample, using the two models. The only unknown parameters are the cementation factor (m) and the Q_v -value.

The distribution of the cementation factors for the two models is given in Figure 2. It is quite evident, that the scatter for the cementation factor from the Dual-Water is much larger than for the Waxman-Smits model. This has been observed before, but in fresh brines the effect on m is exasperated. The Waxman-Smits model gives for the average $m^*=1.716 \pm 0.004$. The Dual-Water model gives for the average $m_0=1.52 \pm 0.03$.

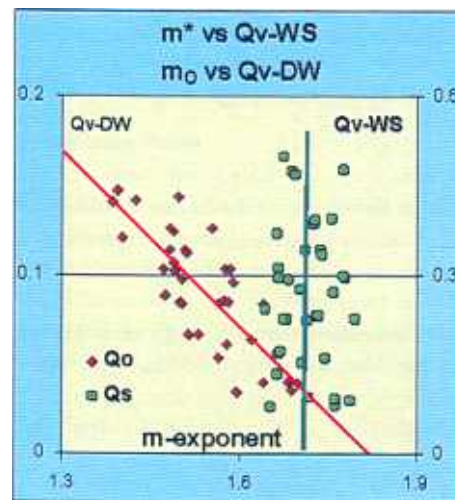


Figure 3: Dependence of m -factor on Q_v for Dual-Water and Waxman-Smits models.

Furthermore it is quite noticeable that the Q_v has a definite effect on the m_0 -value, whereas the Q_v has little effect on the m^* -value (nearly constant). This is shown in Figure 3. We want to reiterate that in Figure 3 both the Q_v -value and the m -factor are determined from two R_0 measurements at different R_w 's using the corresponding model. When we have two R_0 measurements we have only two unknown parameters in equation (6) or (8), i.e. Q_v and m , and we have two equations. So, the results in Figure 3 are self-consistent. Both models assume that the cementation factor is a constant, as long as the pore geometry remains constant, as is the case for the upper Aeolian Sands. These results favour the Waxman-Smits model, which shows a significantly more constant m -factor than the Dual-Water model.

6.2 Irreducible Water Saturation

The Dual-Water model considers the term γQ_v to be the clay bound water saturation. The mobile water saturation is equal to $1 - \gamma Q_v$, when the rock is 100% saturated. It also means that according to the Dual-Water model the lowest S_w measured should be equal or higher

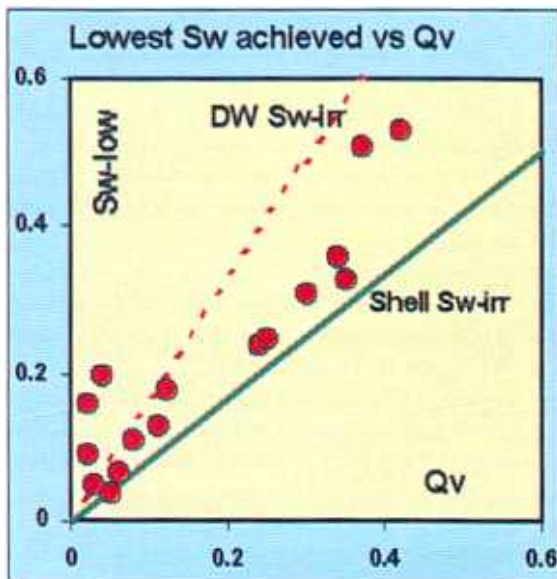


Figure 4: lowest measured S_w in RI experiments.

than γQ_v . These S_{wirr} measurements are available when the Resistivity Index (RI) is measured. In our experiments we have desaturated samples using pressures of up to 15 Bar (220psi).

The lowest water saturations achieved are shown in Figure 4 versus Q_v . The red dotted line is the S_{wirr} predicted by the DW-model and the solid green line the S_{wirr} predicted by the relation given by Klein, Shirley and Hill [4].

$$\gamma = 0.004 / \sqrt{C_{NaCl}} + 0.22 \quad (12)$$

with

C_{NaCl} : Concentration of NaCl (mol/l)

The lowest measured saturations should be larger than the predicted S_{wirr} . It is evident that for these samples the amount of clay bound water is overestimated by the DW-model, but looks acceptable according to equation (12). Equation (12) is not a part of the WS-model, but is always used in conjunction with it.

When we use two R_o -values to determine Q_v , we actually measure BQ_v and because B is known, we may calculate Q_v . However, it has to be realized that B is only an average over a number of samples. So if the actual B is in fact different for a particular sample, the Q_v will be different too. This has no effect on the calculation of the shale effect, because there always BQ_v appears as a product, but it has an effect on S_{wirr} vs. Q_v as in Figure 4.

6.3 Saturation Exponent

At $R_w=0.15 \Omega m$ the factor B_o becomes zero, so X_o equals zero. The DW-model predicts that at $R_w=0.15 \Omega m$ the clay bound water has

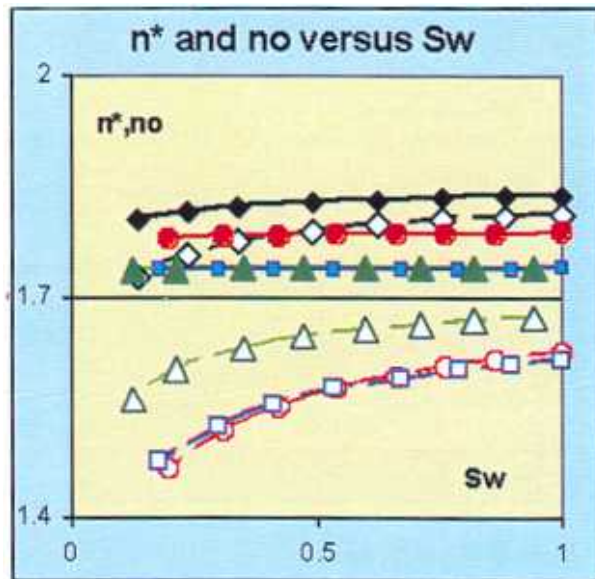


Figure 5: n^* and n_o vs. S_w .

the same resistivity as the bulk water. This means there is no clay effect at this brine resistivity and the actual Q_v value plays no role whatsoever. If n_o is calculated from equation (2) assuming $X_o=0$, and this assumption is correct, then n_o should be constant as a function of S_w . If X is actually greater than zero, n_o will decrease when S_w decreases.

In Figure 5 we have plotted the behaviour of n^* and n_o versus S_w . It shows the fitted n -exponent vs. S_w . The closed symbols show the n -behaviour for the WS-model (n^*), the corresponding open symbols show the behaviour of the DW-model (n_o) for the same samples. There is one sample with a Q_v below 0.1 (diamonds), one with a Q_v around 0.3 and two with Q_v 's around 0.6. The lines result from a fit to the data. The strongest effect occurs with a sample where $Q_v=0.59$ and we clearly see that n_o decreases strongly with S_w , indicating that X_o is much larger than zero. Thus B_o is not zero at $R_w=0.15 \Omega m$.

6.4 DW model is not better

The Dual Water model does not provide a better evaluation of the water saturation than the Waxman Smits model does. In every respect it does actually provide a less reliable picture. It should be realized that the Waxman-Smits model is not correct either, but the DW-model is even less correct. In the following we only will consider the Waxman-Smits model.

7.0 Lab Measurements.

7.1 B-factor

Little data is available to support the WS-model in fresh brines. Waxman and Smits reported data on two groups of samples. Their fit for the B* factor is significantly different for the two groups.

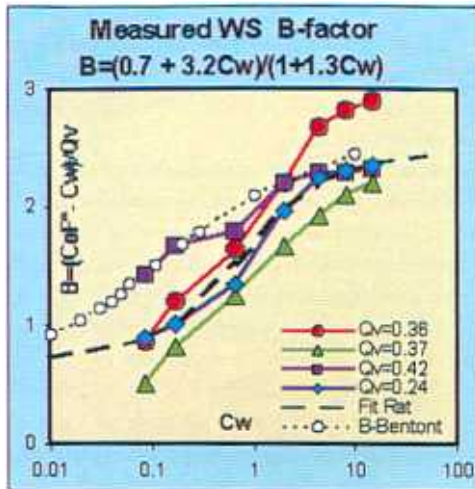


Figure 6: B vs. R_w .

So it was imperative that a better estimate for B* were obtained for the samples of this reservoir. We measured B* as a function of seven different R_w -values on four samples. The results are displayed in Figure 6. Equilibration times of about 4 weeks were used, after the resistivity was changed. The following equation was fitted:

$$B = (0.7 + 3.2/R_w)/(1 + 1.3/R_w) \quad (13)$$

The low C_w asymptote was taken to be equal to the value for a Bentonite suspension (also shown in Figure 6). The high C_w asymptote is taken to be equal to the Waxman-Smits value at 20°C.

7.2 Qv-value

The chemical titration method to measure Q_v is less suitable, because at low values of Q_v a large scatter is always observed, when compared with other methods [7]. This is shown in Figure 7.

We have calculated Q_v using two different brines (R_{w1} and R_{w2}) and the corresponding B-factor (sectn.7.1):

$$Q_v = (1/R_{w2} - Y/R_{w1})/(B_1 \cdot Y - B_2) \quad (14)$$

with

$$Y = R_{o1}/R_{o2}$$

This method becomes less sensitive for $Q_v > 1$, but these values are not important in our evaluation, because at this Q_v -value all water is clay-bound water.

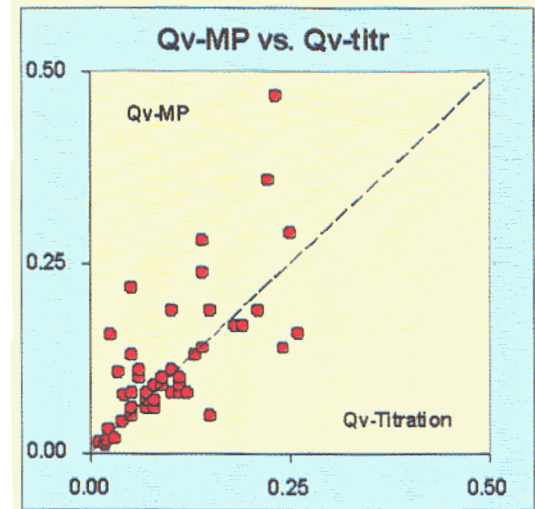


Figure 7: Q_v by Membrane Potential versus Q_v by Titration method.

7.3 Cementation Factor

We first present some original data, before any shale corrections, in Figure 8. We also have drawn a few hypothetical clay-lines, which, to a certain extent, could represent various clay contents. This method could work to some degree. It is not accurate of course. However, we will use the Waxman-Smits model. We do know the value for B from equation (13) and the Q_v -value from equation (14). So, we now may calculate the shale effect $X^* = R_w B Q_v$ and use X^* to calculate:

$$F^* = R_o(1 + X^*)/R_w$$

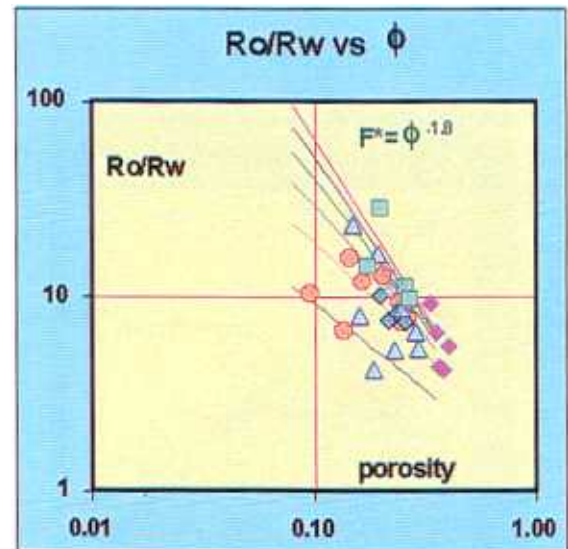


Figure 8: R_o/R_w vs. porosity for Upper and Lower Aeolian Sands.

Plotting F^* versus ϕ on a log-log scale and fitting a straight line through the data will yield a line with a slope of m^* . It was found that the m^* value for different lithologies varied somewhat as is shown in Figure 9 for the upper and lower sands.

The data for the upper sands fall along one line with a slope of $m^*=1.72$, whereas the lower sands fall along a line with a smaller slope.

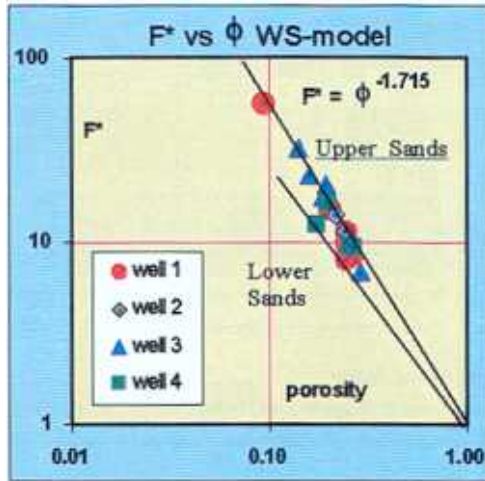


Figure 9: F^* vs. porosity for upper and lower Aeolian Sands.

7.4 Saturation Exponent (n^*)

When we measure the resistivity of a sample that has a water saturation below 100% the effect of the clay minerals is increased. We see in equation (5) that a term X/S_w appears. This means that at $S_w=0.25$ the shale contribution is four times as large. From equations (3) and (5) we see that:

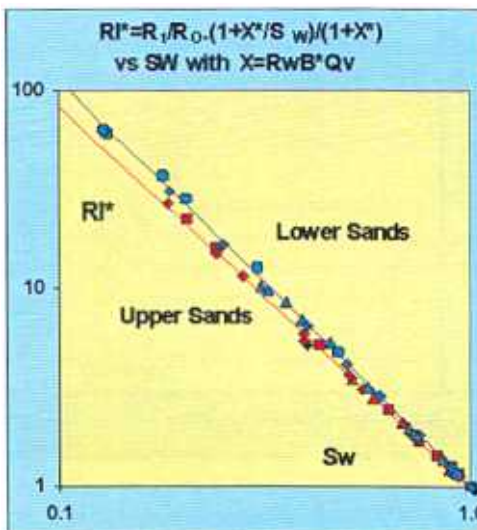


Figure 10: I^* vs. S_w for upper and lower Aeolian Sands.

$$R_t/R_o = I^* \cdot (1 + X^*) / (1 + X^*/S_w) \quad (15)$$

with

$$X^* = R_w B^* Q_v$$

$$I^* = 1/S_w^{n^*}$$

When $I^* = R_t/R_w \cdot (1 + X^*/S_w) / (1 + X^*)$ is plotted versus S_w on a log-log plot we should get a straight line with a slope of n^* . Data for eight samples from the upper and the lower sands are shown in Figure 10. The saturation exponent is different for upper and lower sands.

8.0 Evaluation of Q_v from logs.

All the ingredients, but one are now in place to evaluate the reservoir. We still have to find a way to determine the Q_v -value from logs. This is the critical step for all evaluation models and far outweighs the possible curvature of m^* and n^* . The literature gives five different methods to predict the Q_v -value from log readings. We have adopted two methods and apply those over different sections of the reservoir. The first method is described by Rohuvetz and Fertl [5] and is based on the use of the Spectral Natural Gamma Ray log.

The second method is described by Juhasz [6] and uses the neutron and density porosity difference. Both methods were calibrated in the water logs of all wells in the area, by calculating BQ_v from the electrical logs as:

$$BQ_v = 1/\phi^{m^*} R_o - 1/R_w \quad (16)$$

and correlate this result against the potential Q_v indicators.

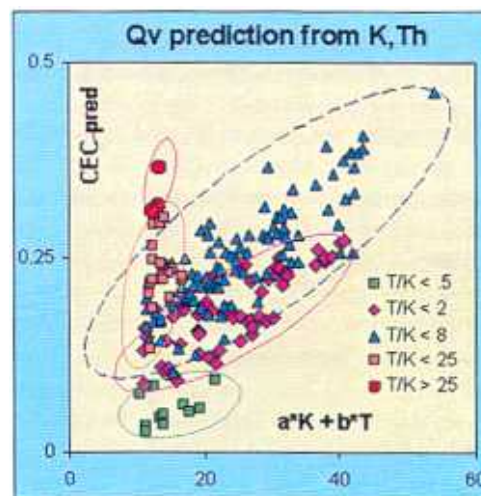


Figure 11: CEC from Spectral Gamma Data.

The Fertl method worked well in the lower and upper Aeolian sands, where the clay composition was rather constant and nearly all the clay was dispersed. Results are shown in Figure 11. It did not work well in the sands where silt and shale laminae were abundant.

The Spectral Gamma Ray tool will yield an indicator for the total amount of Cation Exchange Capacity (CEC) instead of the Cation Exchange Capacity per unit of pore volume (Q_v). However, Q_v and CEC are related as

$$Q_v = \text{CEC} \cdot (1 - \phi) \cdot \rho_{ma}/\phi \quad (17)$$

with

ρ_{ma} : grain density of matrix
 ϕ : total porosity

The neutron density approach worked better in the marine sands, but was not really good. These sands also contain the clay minerals in laminae. A model incorporating the laminated clay distribution in these sands might yield better results, but was not further investigated. There is also a distinct possibility that the R_w in the marine sands is variable.

9.0 Results.

In Figure 12 we show the resistivity and Q_v logs. The resistivity is fully corrected for bore hole effects and thin bed effects. The Q_v is calculated using the method shown in Figure 11. In this case the slope of the line was calculated from the T/K ratio as a continuous function.

In Figure 13 we show the evaluation results, using the Waxman-Smits model, for the upper and lower sands from two wells. Two sections are combined. The first well, to the left, shows a small gas cap at the top, the second well, to the right just reaches the free water level at the bottom. The wells are joined in the middle.

In Figure 13 we show the neutron-density porosity log. The various colours indicate the saturation of fluids filling it. Light blue indicates the saturation of clay bound water (S_{cb}) as calculated using the Klein, Shirley and Hill equation (12). Dark blue indicates the saturation of mobile water. The mobile water saturation follows from the difference in the total water saturation (S_w) calculated using the Waxman-Smits model and the clay bound water saturation as $S_w - S_{cb}$. Green indicates oil and red indicates gas. It is apparent that there is only a very small amount of mobile water in the reservoir. Virtually no water is produced from either well.

In Figure 14 we show the evaluation results, using the Dual Water model, for the same intervals. The colour code is different in this case, to illustrate the incongruous results. Now dark blue indicates the saturation of the total amount of water. Light blue plus dark blue indicate the saturation of clay bound water. This is apparently everywhere larger than the total water saturation. In this Dual Water model evaluation we must use a different value for Q_v . We use equation (16) to calculate the term BQ_v from logs in the water zones. Because B is different so must Q_v be different. We also used the corresponding m_o and n_o values as obtained from the laboratory experiments. The fact that the irreducible water saturation is significantly larger than the total amount of water clearly invalidates

the Dual Water model in fresh water reservoirs. The remainder of the porosity is again filled with oil (green) or gas (red).

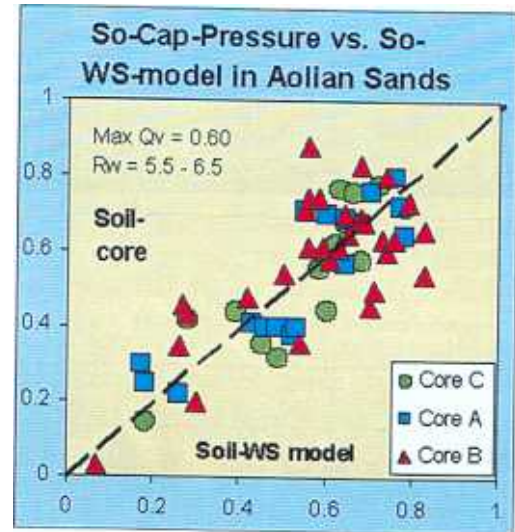


Figure 15: Comparison of Oil saturations from the Waxman-Smits model and from averaged Capillary Pressure curves.

A good evaluation should yield water saturations that are in accordance with Capillary Pressure data. As the oil is rather light and the temperature rather low, the conversion of Hg-Cap Curves to field conditions is not difficult. In Figure 15, we plotted Cap-Pressure S-oil versus WS-model S-oil. The Cap Pressure saturations were calculated from averaged type curves. The scatter in Figure 15 is the result from using averaged type curves, which are determined using the porosity as the type parameter. Cap Curves are hardly dependent on porosity, but much more on permeability. This will introduce the scatter. However, the slope of the correlation line is clearly one. This of course should always be the case, when both types of laboratory tests are performed correctly.

Figure 14: Dual Water Model Evaluation Results

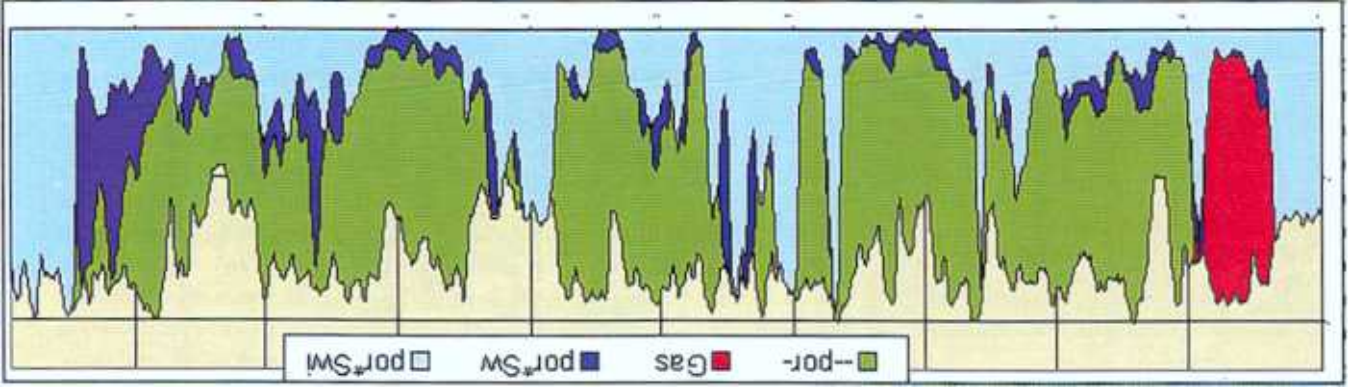


Figure 15: Wecover Smith Evaluation Results

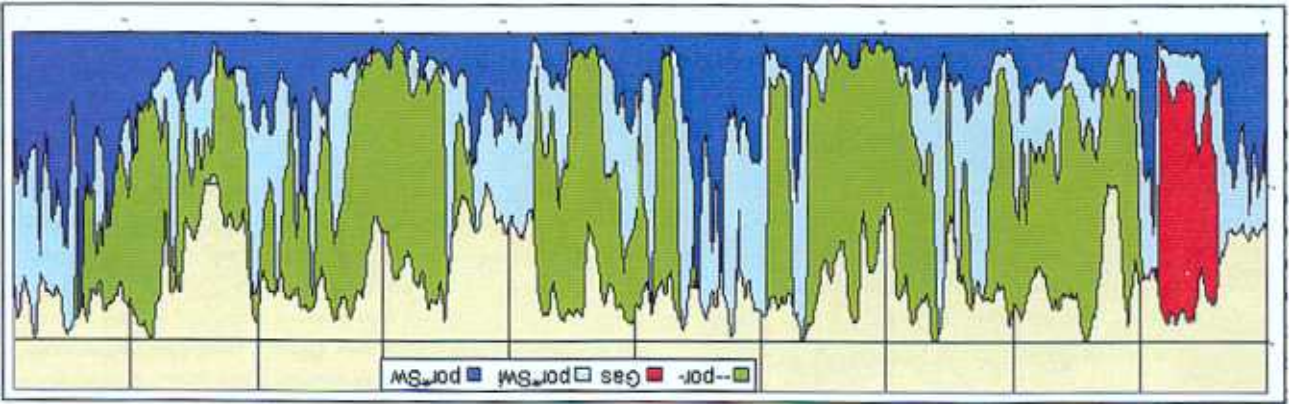
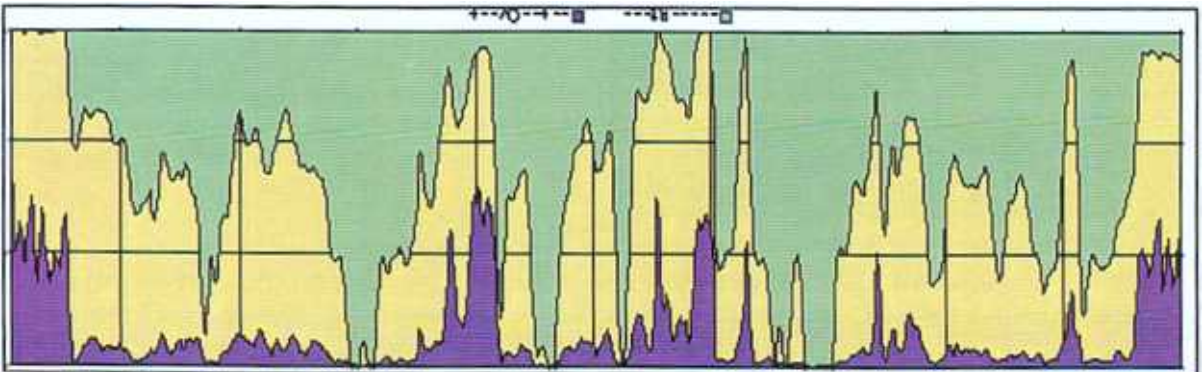


Figure 12: Resistivity and Q_r vs. depth



10.0 Discussion.

The adapted WS-model (only a different equation for the B-factor is used) yields good results for the sections with dispersed clays. The sections with laminated clays should be evaluated using a model for laminated clays. The marine sands may have another evaluation problem: we now think that the resistivity of the brine in the marine sands may be variable, because of poor lateral connectivity in these sections. This possibility was considered as a solution in our attempts to reconcile the water saturations derived from electric logs and cap curves. So the evaluation of the marine sands is significantly more complicated than that of the Aeolian sands.

The DW-model fails in fresh brines because it is intrinsically contradictive. By using only one geometric constant (F) it assumes that the clay is infinitely fine dispersed throughout the pore space. Once this assumption is made a layer of clay bound water can no longer be assigned to the clay, because this would fill the whole pore space with clay bound water. A geometric model allowing for a clay bound water layer needs two additional geometric constants and is too unwieldy to ever become practical. Furthermore, the vague notion of a constant brine resistivity within the clay bound water is not supported in the literature, not even in the literature quoted by CCD (Ref 3). CCD arrived at their conclusion from observations in shales. However, most often it is found that the salinities in shales is within 1/4 to 1/2 of the salinity in the associated sands, while it is much higher very close to the sands. Furthermore, CCD extrapolate this unsubstantiated notion from compacted shales to dispersed clays.

The WS-model is not irrefragable either. It is valid only for infinitely small amounts of dispersed clay. However, realistic amounts of clay are still well described using the WS-model. All deficiencies pale with respect to the inaccuracy in estimating Qv from logs.

References.

1. Worthington, P.F.; (1985)
The Log Analyst January-February 23-40
The Evaluation of Shaly-Sands Concepts in Reservoir Evaluation
2. Waxman, M.H., Smits, L.J.M.; (1968)
Soc. Pet. Engrs. J. 8, 107-122
Electrical Conductivity In Oil-bearing Shaly Sands.
Waxman, M.H., Thomas, E.C.; (1974)
Soc. Pet. Engrs. J. 14, 213-225
3. Clavier, C., Coates, G., Dumanoir, J.; (1977)
SPE Paper 6859, also
Soc. Pet. Engrs. J. (1984)
Theoretical and Experimental Basis for the Dual Water Model for the interpretation of Shaly Sands.
4. Klein, G.E., Hill, H.J., Shirley, O.J. (1979)
The Log Analyst 20, May-June
Bound Water in Shaly-Sands, Its relation to Qv and Other Formation Properties.
5. Ferti, W.H., Rubovetz, N., (1981)
Dresser-Atlas Reprint 12/81 2m 9454
Digital Shaly-Sand Analysis Based on
Waxman-Smits Model and Log Derived Clay Typing.

6. Juhaz, I. (1979)
Trans. 20th SPWLA logging Symposium, June 3-6
The Central Role of Qv and Formation- Water Salinity in the Evaluation of Shaly Formations
7. Thomas, E.C.; (1976)
J. Pet Techn. Sept., 1087-1096,
The Determination of Qv from Membrane Potential Measurements on Shaly Sands.

Author

Rob T. Wittebrood consults in petrophysics. He specializes in the areas of Electrical Properties, Natural Spectral Gamma Ray and Capillary Pressure. He works with various laboratories in the Calgary area. He holds separate degrees in Chemical Engineering and Engineering Physics. He worked for ten years at the Technical University of Delft in Holland. He also worked twenty years for Shell, mainly in research, at various locations and in various positions.

Appendix A.

In the original paper introducing the Dual Water model, the authors present their model as equation (12), which we reproduce here as equation (A1):

$$C_o = [(1 - \alpha v_Q \cdot Q_v) C_w + \beta \cdot Q_v] / F_o \quad (A1)$$

With

$$\beta = 2.05 \text{ cc/meq}/\Omega m$$

$$v_Q = 0.3 \text{ cc/meq}$$

$$\alpha = 1 \quad R_w < 0.3$$

$$\alpha = 1 + 1.441 \cdot (R_w - 0.3)^{2/3} \quad R_w > 0.3$$

The last equation is our fit to the data given in Ref. 3. α describes the expansion of the double layer at the clay surface with decreasing salinity.

The two terms on the RHS with Qv can be combined, resulting in:

$$C_o = [C_w + (\beta - \alpha v_Q C_w) Q_v] / F_o$$

We now divide the LHS and RHS by Cw:

$$C_o / C_w = [1 + (\beta / C_w - \alpha v_Q) Q_v] / F_o \quad (A3)$$

Replacing the conductivity by the resistivity ($R=1/C$) we get:

$$R_w / R_o = [1 + (\beta R_w - \alpha v_Q) Q_v] / F_o$$

Inverting this equation yields:

$$R_o / R_w = F_o / [1 + (\beta R_w - \alpha v_Q) Q_v]$$

We take the factor Rw outside of the brackets to get:

$$R_o / R_w = F_o / [1 + R_w (\beta - \alpha v_Q / R_w) Q_v] \quad (A6)$$

This may be written as:

$$R_o/R_w = F_o/[1 + R_w B_o Q_v] \quad (A7)$$

with

$$B_o = (\beta - \alpha v_Q/R_w) \quad (A8)$$

as α and v_Q always appear as their product we have replaced them by one symbol γ to get:

$$B_o = (\beta - \gamma/R_w) \quad (A9)$$

Equation (12) in Ref (3) is rewritten as equation (13) to show, that if F_o is independent of Q_v , then F^* must be dependent on Q_v and vice versa. However, for these samples the effect appears only at very high values of Q_v , where the shale content must be very large and the pore geometry of the samples can not be the same as for low Q_v -values. The authors did not have access to the lithological description of the samples and did not realise this lithological effect. Furthermore, in our Figure (3) we show that the DW-model m_o depends much stronger on Q_v than m^* . This is in strong contrast with Figure (3) in Ref. (3).

The Dual Water model gets its numerical values for γ and β in equation (11) from a curve fit to WS-data shown in their Figure 4 and our Figure A1. The curvature in the group (I) data, is attributed to the effect of clay bound water. The data is fitted using:

$$C_x = \beta Q_v / (1 - \gamma Q_v) \quad (A10)$$

Where γQ_v is interpreted as the fraction of clay bound water. This fit is the only source of the values for β and γ , and is the crux of the DW model. Equation (A10) is incorrect. First, the effect is due to a difference in lithology at high clay contents. Waxman and Smits restricted their fit to Q_v values below 1 with the assumption that m^* is independent of Q_v and R_w . If m^* is not constant, then the WS-Figure (4) is incorrect. Thus, the fit used in the DW-model would be inappropriate and the DW-model would not hold. If m^* is constant, the DW-model is not correct per se. So, the DW model is based on an incorrect assumption or incorrect data.

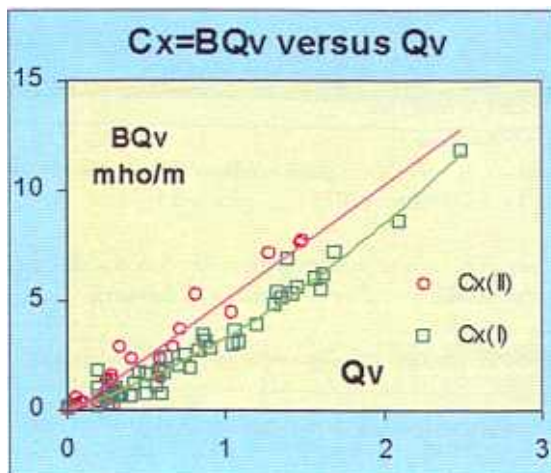


Figure A1: BQ_v versus Q_v for WS-data from group I and group II, as published in Ref(2) and Ref(3) (visual-copied).